On the tribological behavior of cobalt-based nanocomposite coatings containing ZnO@Graphene oxide core-shell nanoparticles

Manuelle Romero, Valdicleide Mello, Christine Boher, André Tschiptschin, Cherlio Scandian

On the tribological behavior of cobalt-based nanocomposite coatings containing ZnO@Graphene oxide core-shell nanoparticles

Manuelle Romero [a,*], Valdicleide Mello [a], Christine Boher [b], André P. Tschiptschin [c], Cherlio Scandian [a]

[a] *Laboratory of Tribology, Corrosion and Materials (TRICORRMAT), Department of Mechanical Engineer, Federal University of Espírito Santo, Av. Fernando Ferrari, 514, Vitória, 29075-910, Brazil*

[b] *Institut Clément Ader (ICA), Université de Toulouse, Mines Albi, SUMO, OM04, Campus Jarlard, F-81013, Albi, France*

[c] *Metallurgical and Materials Engineering Department, Polytechnic School of the University of Sao Paulo, Av. Professor Mello Moraes, 2463, Sao Paulo, 05508-030, Brazil*

A hybrid nanocrystalline cobalt-based coating was prepared by cathode plasma electrolytic deposition (CPED). Zinc oxide and graphene oxide (GO) nanoparticles were mixed to form a core-shell structure through electrostatic self-assembly by using (3-aminopropyl)triethoxysilane (APTES) modifier. ZnO@GO nanoparticles were used as additives to improve wear and friction properties of deposited coatings. The concentration effect of core-shell ZnO@GO addition (0.1, 0.2 and 0.3 %wt) on the friction, wear, coating thickness and mechanical properties was investigated. The composition and microstructure of deposited coatings were studied by scanning electron microscope (SEM), X-ray diffraction (XRD), Raman spectroscopy and energy dispersive spectroscopy (EDS). Reciprocating sliding wear tests using a ball-on-plate configuration were carried out on a PLINT TE67 tribometer. AISI 52100 steel was used as ball and the coating deposited onto a AISI 304 stainless steel substrate was used as plate. Coatings were dense, nanocrystalline and uniform with a FCC metastable cobalt structure. Core-shell concentration above to 0.2 %wt resulted in a decrease of grain size and an increase of hardness and wear resistances. Nanoparticles act as nucleation sites for grain formation, decreasing grain sizes. Samples using 0.3% ZnO@GO displayed the lowest wear and friction coefficients. ZnO@GO nanoparticles enables the formation of a protective layer consisting of oxide and exfoliated GO on the top of worn surfaces.

1. Introduction

Cobalt is an important engineering material with high wear and corrosion resistances. Its unique properties such as high hardness, biocompatibility and magnetic properties justifies its use in microelectronics, sensor technology and in the defense industry [1–3]. Multiple methods have been used to deposit cobalt coatings, but among them cathodic plasma electrolysis deposition (CPED) stands out due to its high deposition rates, no need for electrolyte additives and to the deposition of nanocrystalline coatings with high hardness and adhesion. CPED emerges as a result of the combination of conventional electrolysis with atmospheric plasma processing [4,5].

Cobalt and nickel coatings are eco-friendly alternatives to conventional chromium deposits which uses hazardous and source of pollution hexavalent chromium plating [6–8]. However, cobalt outstands nickel due to its better tribological response with an increase resistance to adhesion and delamination wear, resulting in lower and stabler friction coefficient compared to nickel [8,9]. Furthermore, cobalt has an excel-lent thermal stability [10,11].

Nanoparticles (NPs) have been used in electrodeposition process in order to improve mechanical, wear and corrosion resistances [12]. NPs increase nucleation sites and hinder crystal grow, resulting in smaller grain sizes and in higher hardness [11]. A reduction of pore fraction is also expected, which improves corrosion resistance by prohibiting cor-rosive ions to enter [13].

Different composite cobalt-based coatings had been deposited using different particles such as SiC [10], carbon nanotubes [14], TiO_2 [2] and WC [15] in order to decrease wear and corrosion. Liu et al. [11] added graphene oxide (GO) NPs to cobalt coating using conventional elec-trolysis process. The authors observed that GO addition affected the

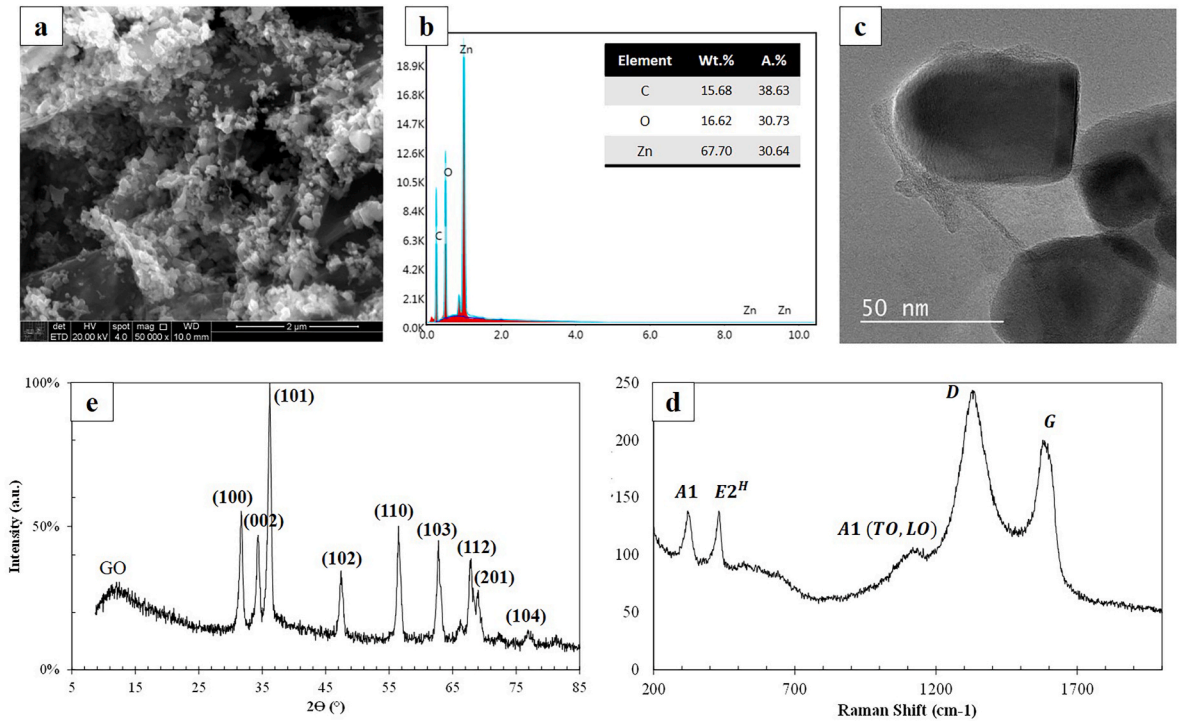

Fig. 1. (a) SEM image, (b) EDS spectrum, (c) TEM image, (d) XRD pattern and (e) Raman spectrum of ZnO@GO core-shell nanoparticles.

morphology of deposits, leading to grain refinement, hardness increase and friction reduction (from 0.65 to 0.33). While cobalt pure exhibited severe adhesive wear, the coating with embedded GO showed abrasive wear and mild adhesive wear.

Toosinezhad et al. [13] electrodeposited Co/graphene coatings on ST37 steel substrate. Graphene was successfully distributed within the matrix and 0.2 g/L content led to the best tribological response, reducing the friction in 1.6 times and wear in 5.5 times compared to Co pure film. Besides, surface morphology depended on concentration, increasing graphene content morphology changed from pyramidal grains to needle shape grains.

NPs addition in CPED process has also been reported. Huang et al. [16] added Mo_2S nanoparticles to form a Ti(C,N) based composite with outstanding lubricating properties. The authors observed that Mo_2S weaken electrolyte capacity to cool the sample during CPED as it reduces electrolyte flowing capacity.

Liu et al. [17] observed that SiC nanoparticles positively affected the electrical behavior of CPED when depositing Al_2O_3 composite coatings. The destructive effect of plasma breakdown is diminished, resulting in a smoother and wear resistant coating. Furthermore, the authors under-lined that friction and wear only decrease for appropriate NPs concen-trations. Quan et al. [18] showed that the addition of Y_2O_3 NPs to Ni–Cr based electrolytes enabled Cr_2O_3 growth in a very small scale, greatly increasing corrosion resistance.

There is a lack of literature concerning the use of core-shell nanoparticles as additives to electrodeposited coatings. These particles show a synergistic effect on the tribological contact. The hard core supports the normal load while the soft shell works as a solid lubricant. In this work, cobalt-based coatings using different contents of core-shell ZnO@GO core-shell NPs as additives were deposited by CPED. The tribological behavior of those hybrid coatings were investigated and the influence of core-shell NPs addition on wear and friction was scruti-nized. Mechanical properties, microstructure and surface topography were also investigated.

2. Experimental

2.1. Preparation of ZnO@GO core-shell NPs

GO was synthetized from natural graphite powder by a modified Hummers' method [19]. 1 g of graphite and 0.5 g of $NaNO_3$ were added to 70 ml of H_2SO_4 and stirred in an ice bath. 3 g of $KMnO_4$ was slowly added to the solution and stirred for 2 h. Then, 3 ml of 30% H_2O_2 was gradually added and the solution was diluted with distilled water. The solid product was collected after washing and centrifugation. The product was dried at 60 °C for 24 h. In order to obtain core-shell ZnO@GO NPs [20], firstly, 1 g of ZnO NPs (50 nm spherical-shaped nanoparticles supplied by Sigma-Aldrich) were dispersed in a mixture of 45 ml distilled water and 105 ml ethanol, stirred, and then mixed with 0.2 g of (3-aminopropyl)triethoxysilane (APTES) (99%, ChemImpex) to functionalize ZnO surface with positive amino groups. The solution was stirred for 7 h at room temperature (21 °C) to complete hydrolysis of APTES. Functionalized ZnO nanoparticles were centrifuged, washed and dried at 80 °C for 15 h.

Core-shell ZnO@GO NPs [21] were prepared by electrostatic self-assembly. 0.5 g of GO was added to a mixture of 700 ml distilled water and 35 ml of ethanol. The solution was sonicated for 20 min and stirred for 40 min to produce a well-dispersed solution. Then, 1 g of functionalized ZnO was added to the solution and stirred for 1 h. The final ZnO@GO were washed, centrifuged and dried at 70 °C for 24 h.

2.2. CPED of cobalt-based coatings

A DC power supply (0–120 V) was used and a data acquisition system connected to a computer was used to monitor current and voltage. The electrolyte was recirculated and cooled by using a 200 l/h flow rate pump and an iced bath, respectively. Electrolyte temperature was monitored during the process using a thermocouple. A graphite (99.9% purity) plate was used as the anode and the anode-cathode distance was 30 mm. Austenitic stainless-steel AISI 304 plate samples were used as cathode. Samples were grounded to a 1200 grit, ultrasonically cleaned with acetone for 15 min. Deposition area was bounded and fixed in 1

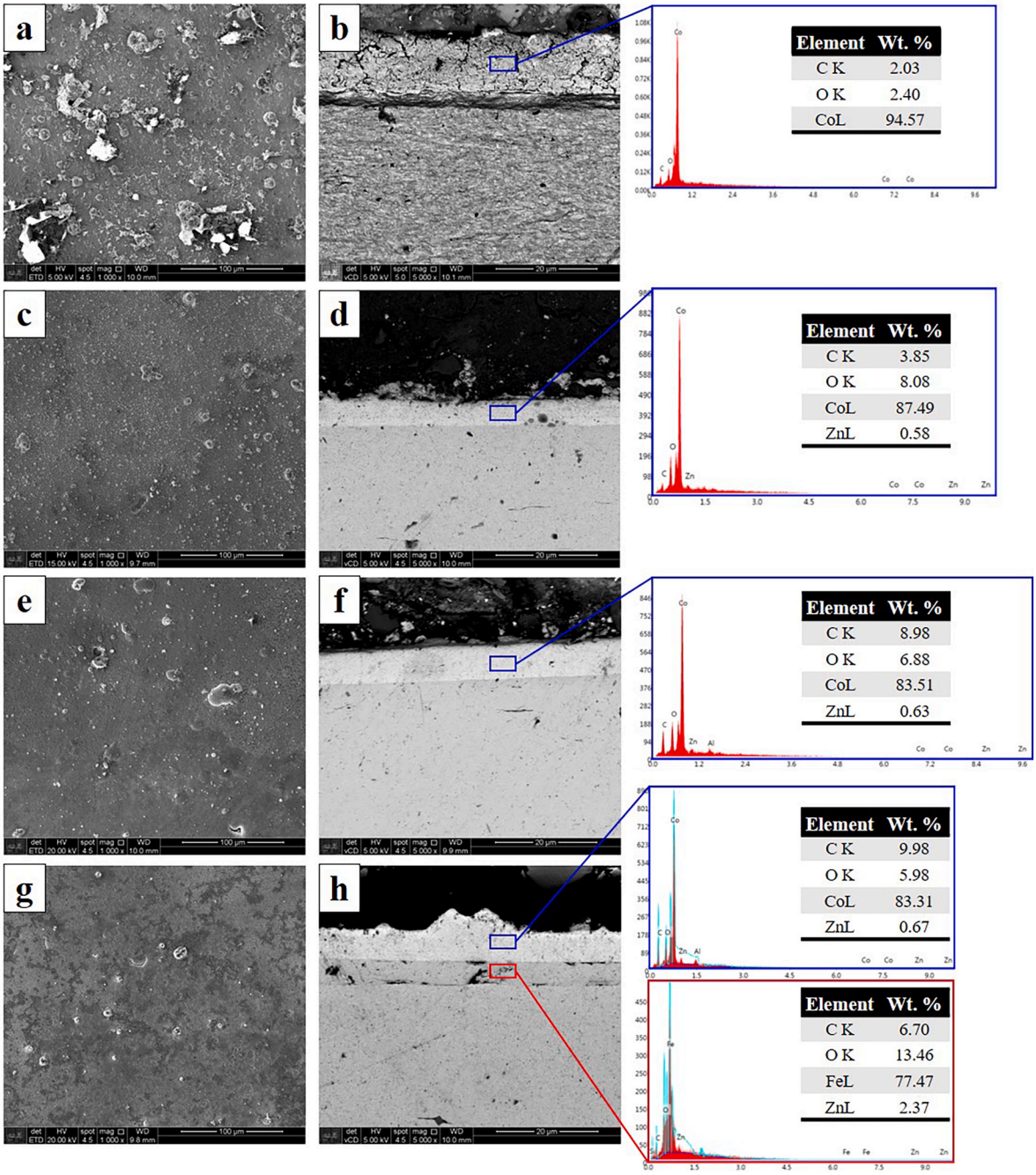

Fig. 2. SEM images of deposited coatings by CPED: Co (a) surface (b) cross-section, Co0.1 g/L ZnO@GO (c) surface, (d) cross-section, Co0.2 g/L ZnO@GO (e) surface (f) cross-section, Co0.3 g/L ZnO@GO (g) surface (h) cross-section. EDS analysis of coatings are in detail.

cm^2 by an ABS polymer holder. The electrolyte consisted of $CoSO_4.7H_2O$ (25 g/l), H_2SO_4 (60 g/l) and distilled water was used as solvent. To deposit Co ZnO@GO hybrid coatings, ZnO@GO NPs were added to the electrolyte in different content (0, 0.1, 0.2, and 0.3 g/L). Ultrasonic sonication during 30 min prior to deposition and electrolyte recircula-tion ensure the homogenizing of the electrolyte. Deposition was carried out at 85 V for 3 min.

2.3. Characterization

ZnO@GO nanoparticles were characterized by Raman spectroscopy in a LabRam HR Evolution spectrometer, using a 633 nm laser, 50x objective and 90 mW laser power. X-ray diffraction (XRD) were carried out on a Rigaku Ultima diffractometer using molybdenum radiation ($\lambda = 7.0926$ nm) to identify each phase. A FEI-Inspect F50 field-emission scanning electron microscopy (FESEM) with an X-ray energy dispersive spectrometer (EDS) and Transmission electron microscope (TEM) were used to evaluate NPs morphology, size and composition.

Co and Co/ZnO@GO coatings were characterized by XRD and Raman spectroscopy. An 3D optical profilometer (SNeox, Sensofar) was used to evaluate surface topography. FESEM imaging was carried out to investigate surface morphology and coating thickness while EDS was used to analyze the composition of the coatings. Vickers microhardness tests were carried out using a load of 25 gf. Ten indentations were done in each sample.

Ball-on-plate sliding tests were carried out on a PLINT TE67 tribometer (Phoenix Tribology Ltd) using the AISI 304 coated samples as the plate and an AISI 52100 steel as the ball. Reciprocating wear tests were

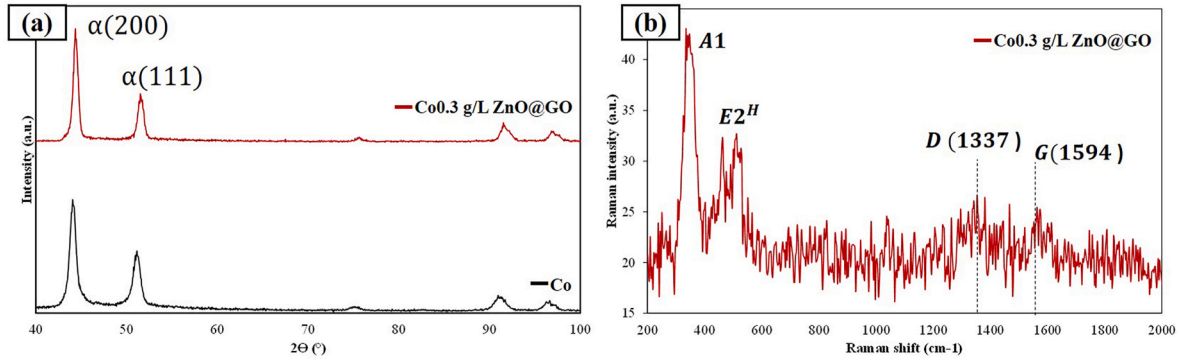

Fig. 3. (a) XRD patterns of Co and Co0.3 g/L ZnO@GO (b) Raman spectrum of Co0.3 g/L ZnO@GO.

suitable due to the sample plate size. The screened area is limited to a region with uniform deposited layer. The apparatus used to CPED is limited in terms of current, thus to achieve the required deposition density current, a small area of 1 cm^2 was selected. Besides, the alternating stresses promoted in this test have been effectively used to test the tribological behavior of coatings [9,16,22,23].

Tests were performed with a stroke length of 2.5 mm, a sliding frequency of 3 Hz and a normal load of 500 N. The initial Hertz contact pressure was 0.7 GPa. Test duration was 30 min. Friction force was monitored throughout the test using a load cell with 10 Hz acquisition frequency. Ball and plate were ultrasonically cleaned with acetone for 15 min prior the test. Tests were performed in a random order.

Mass loss was determined using an analytical balance with 0.1 mg precision. After wear tests, main wear micro-mechanisms were determined by FESEM image analysis of the wear track. Tribolayer formation on the wear track was evaluated by EDS.

3. Results and discussion

3.1. Characterization of ZnO@GO nanoparticles

Fig. 1 shows SEM image, TEM image, EDS spectrum, XRD pattern and Raman spectrum of ZnO@GO nanoparticles prepared in this experiment. It can be seen in Fig. 1 that ZnO nanoparticles are imbedded in GO layers, forming a nanocluster and EDX results confirms Zn, C and O presence. Fig. 1c confirms that ZnO nanoparticles were successfully coated with a thin GO layer, resulting in a core-shell nanostructure. The diffraction pattern depicted in Fig. 1d shows a wide peak at 11.2° correspondent to GO [24] and several ZnO peaks indicating the forma-tion of hexagonal wurtzite phase [25]. Fig. 1e shows Raman spectrum of ZnO@GO nanoparticles exhibiting two characteristic peaks of GO at 1337 cm^{-1} and 1584 cm^{-1}, which correspond to disordered D band and crystalline G band, respectively [24,25]. The intensity ratio of the D band and G band (I_D/I_G) is 1.22. The spectrum also reflects the formation of hexagonal wurtzite. Peaks at 339 cm^{-1} corresponding to A1 vibration mode, at 441 cm^{-1} representing E2 high non-polar mode and a broad band at 1154 cm^{-1} corresponding o the A1 transversal optical (TO) and longitudinal optical (LO) modes [26] are present.

3.2. Morphology and microstructure of the coatings

SEM images of surfaces and cross-sections and EDS analysis of Co and Co/ZnO@GO composite coatings are shown in Fig. 2. Pure Co coating exhibited a porous and rough microstructure. Cross-section image shows a higher thickness when compared to composite coatings, but micro-cracks are clearly seen. A spheroidal nodule morphology is observed in all coatings, which is derived from the subsequent implosion and quenching of surfaces [27]. However, with nanoparticle addition, nod-ules are smaller and surfaces are smoother. Nanoparticles can act as new nucleation sites and hinder crystal growth process [11,13]. EDS analysis confirms the deposition of ZnO@GO nanoparticles along the cobalt matrix. The content of carbon, oxygen and zinc increase with the content

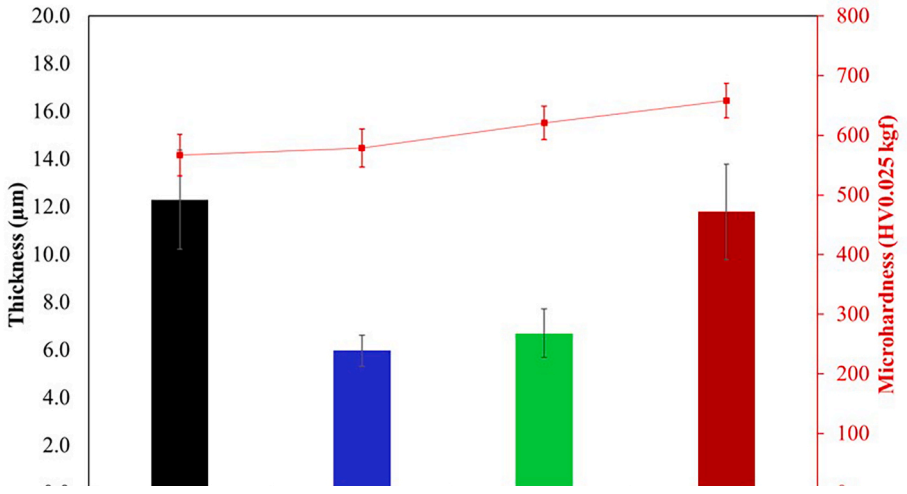

Fig. 4. Thickness and microhardness of Co, Co0.1 g/L ZnO@GO, Co0.2 g/L ZnO@GO and Co0.3 g/L ZnO@GO.

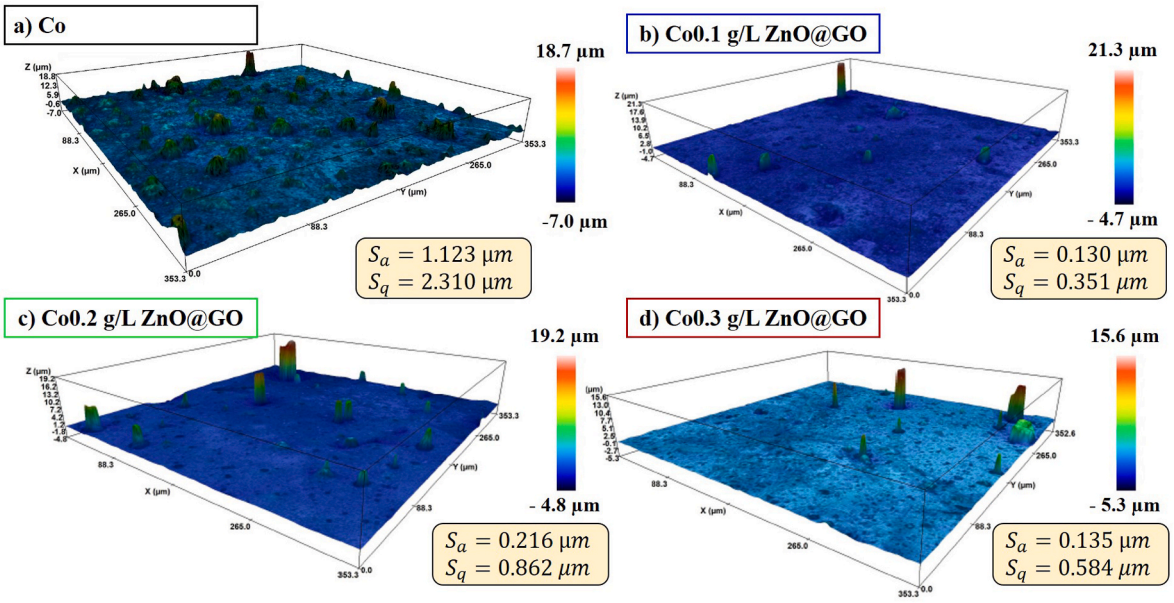

Fig. 5. 3D profilometry results of Co, Co0.1 g/L ZnO@GO, Co0.2 g/L ZnO@GO and Co0.3 g/L ZnO@GO. S_a and S_q roughness parameters are displayed.

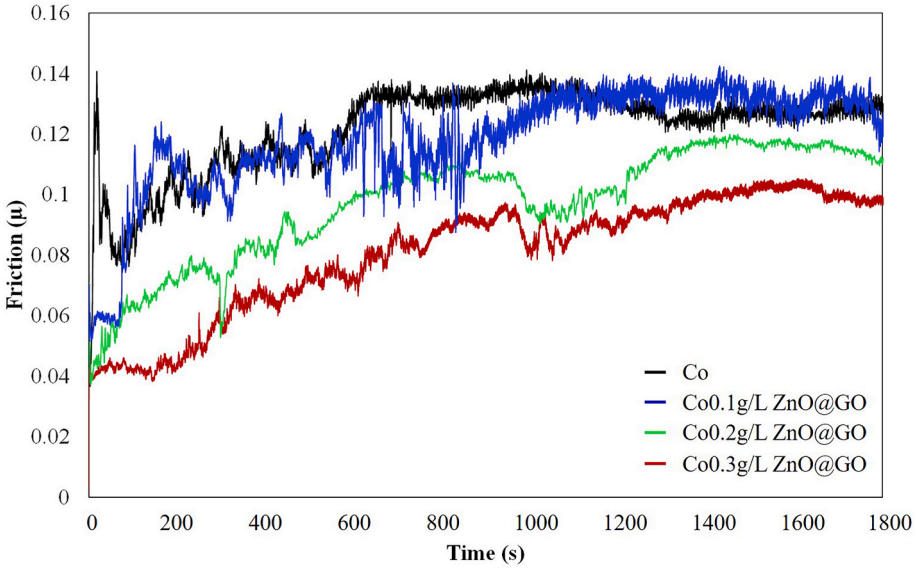

Fig. 6. Friction coefficient curves for Co, Co0.1 g/L ZnO@GO, Co0.2 g/L ZnO@GO, Co0.3 g/L ZnO@GO.

of ZnO@GO added to the electrolytic bath. Besides, coatings with high-purity were obtained, since no additives were required. Using 0.3 g/L of ZnO@GO, a double layer was formed. A thicker top layer composed of Zn, C and O in a cobalt matrix was formed and a bottom layer composed of the same elements of the core-shell nanoparticles, but in an iron matrix. From these results, it can be proposed that at higher contents, more ZnO@GO is available, migrating faster and nucleating first. By the action of plasma, local melting occurs and nanoparticle are incorporated into the iron matrix, forming an iron-based coating. With the progression of plasma process, cobalt ions also migrate, enabling the cobalt-based coating formation.

Fig. 3 a shows diffraction patterns of the Co and Co0.3 g/L ZnO@GO. Both coatings display strong metastable face-centered cubic (FCC) α(200) and α(111) peaks [28], differently from coatings deposited through traditional electrolysis methods, which typically show hexag-onal compact (HCP) structure [8]. In addition, peak broadening is observed in both samples indicating nanograin formation. Average grain size was calculated using Scherrer's equation from XRD patterns, Co has 20.1 nm grains and Co0.3 g/L ZnO@Go has 18.7 nm grains. During CPED grains are nucleated and subsequently quenched by the cool electrolyte, promoting nanograins and metastable microstructures for-mation [27]. Besides, when 0.3 g/L ZnO@GO was added, it resulted in grain refinement and, consequently, microhardness increase, as can be seen in Fig. 4 [22].

Thickness of coatings (Fig. 4) were also affected by nanoparticles addition. 0.1 and 0.2 g/L ZnO@GO addition decreased coating thickness, but at the same time produced more even and smoother coatings. 0.3 g/L of ZnO@GO addition resulted in a double layer, iron-based and cobalt-based, with thickness similar to the Co coating. Raman spec-troscopy results of Co0.3 g/L ZnO@GO confirms ZnO peaks at 339 cm^{-1} and 441 cm^{-1} and broad GO D 1337 cm^{-1} and G 1594 cm^{-1}.

3D profilometry results (Fig. 5) shows that composite coatings are smoother, displaying smaller S_a and S_q topography parameters. Nanoparticle addition was effective in decreasing porosity and roughness.

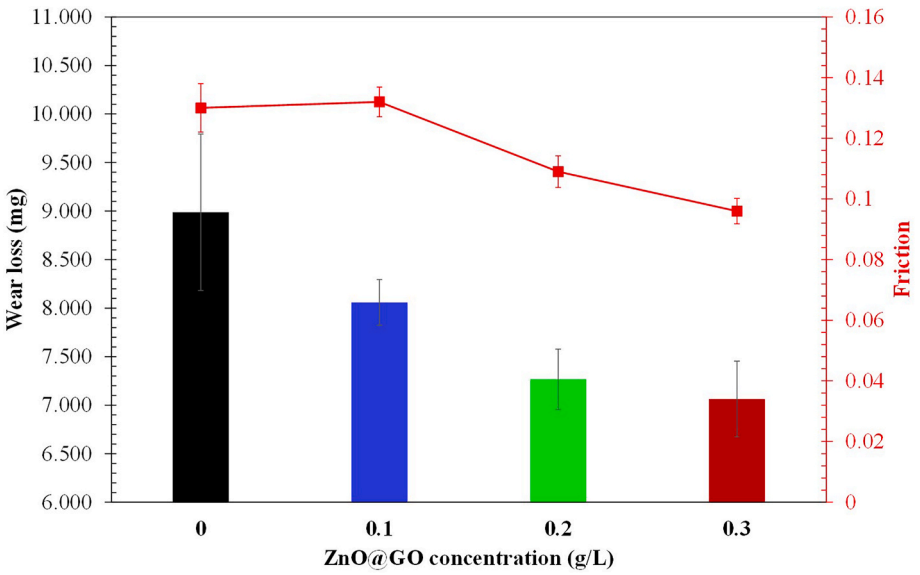

Fig. 7. Wear loss for Co, Co0.1 g/L ZnO@GO, Co0.2 g/L ZnO@GO, Co0.3 g/L ZnO@GO sliding in air against AISI 52100 steel ball under a normal load of 500 N.

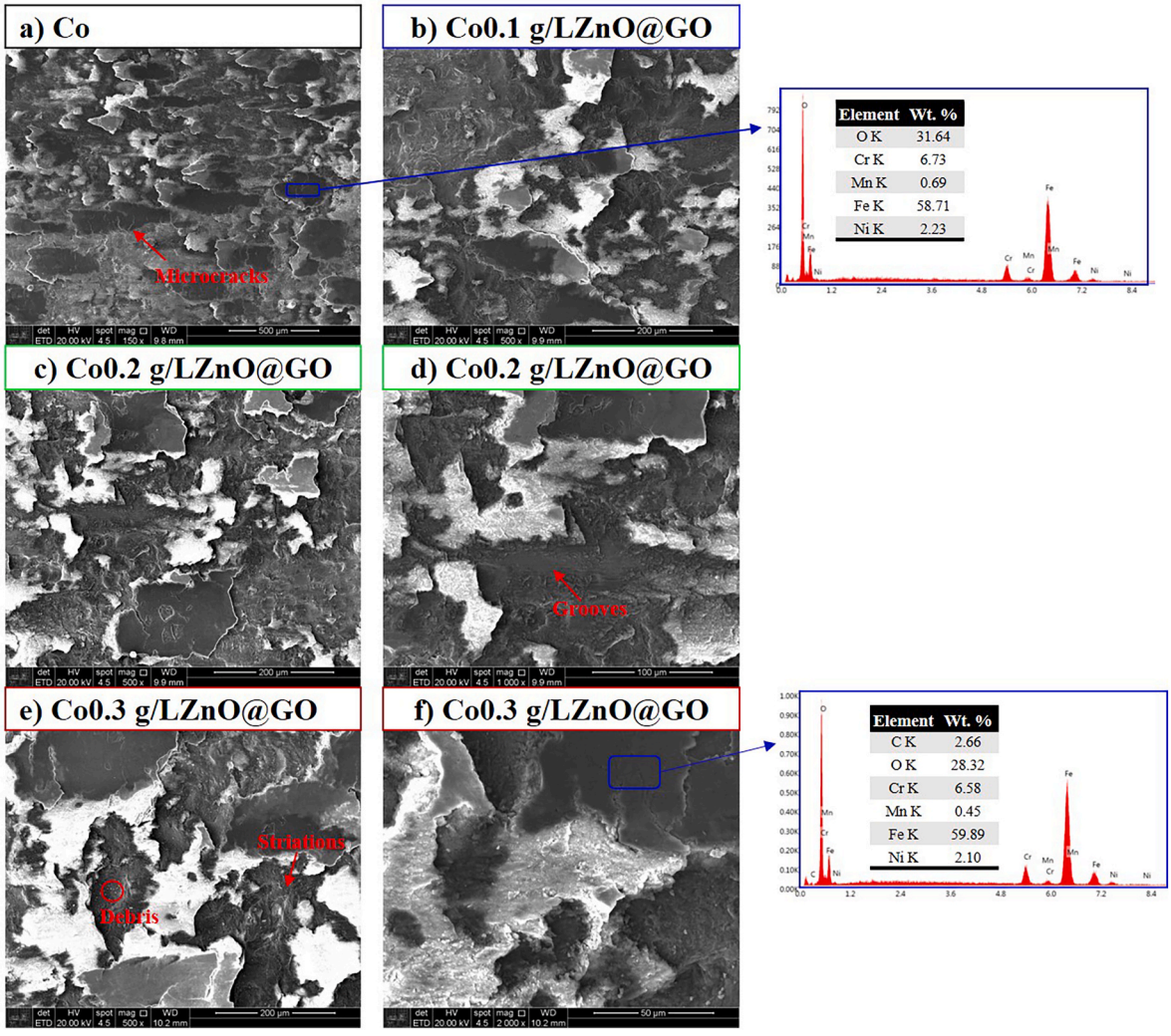

Fig. 8. Worn surface of (a) Co, (b) Co0.1 g/L ZnO@GO, (c,d) Co0.2 g/L ZnO@GO, (e,f) Co0.3 g/L ZnO@GO sliding against AISI 52100 ball under a load of 500 N.

3.3. Tribological results

Friction coefficient curves of Co and Co composite coatings are shown in Fig. 6. Friction coefficient of Co coating increases with time, reaching 0.12 after 700 s. This friction level is maintained throughout the rest of the test. Co0.1 g/L ZnO@GO coatings displayed the same trend and friction coefficient as pure Co coatings. However, when adding higher amounts of nanoparticles, composite coating exhibited reduced friction coefficient. Both, Co0.2 g/L ZnO@GO and Co0.3 g/L ZnO@GO friction curves had prolonged running-in periods (1200 s) and lower steady-state friction coefficient. 0.3 g/L of nanoparticles addition resulted in the lowest friction coefficient (0.09) against the steel ball.

The wear loss of the coatings during the tests are summarized in Fig. 7. Compared with ZnO@GO free Co, the wear of Co0.2 g/L ZnO@GO and Co0.3 g/L ZnO@GO were reduced 20% and 22%, respectively. The wear loss of Co0.1 g/L ZnO@GO was similar to Co coatings, the difference is between error bars. GO nanoparticles are known as excellent solid lubricant, which reduce friction and wear [11, 23]. Moreover, the addition of core-shell nanostructures which possess the synergy of the ZnO hard core and the GO flexible shell are probably responsible for the improved wear and friction properties of Co0.2 g/L ZnO@GO and Co0.3 g/L ZnO@GO [25].

As shown in Fig. 8, all deposited coatings exhibited severe plastic deformation, denoting adhesive wear. A tribo-layer formation is observed in the top of Co coatings. EDS analysis indicates that this build- up is high in oxygen and iron. Microcracks are seen inside this layer, which lead to the detachment of large oxide particles alongside with bulk material. The lower positions of the sample surface are regions with actual metal-metal contact and are severely deformed. During wear, oxide material of the ball can be transferred to the plate due to the severe contact conditions. Besides, in some regions, the Co coatings is also removed, exposing the substrate. This removed material is mixed with the iron oxide transferred material, forming a tribo-layer that contrib-utes to reduce the friction coefficient of the tribo-pair.

Co composite coatings displayed similar wear mechanisms. Co0.2/L ZnO@GO and Co 0.3 g/L ZnO@GO coatings also exhibited the formation of oxide layer. However, the lower positions are less deformed. Striation marks can be observed as a result of the consecutive cycles of plastic extrusion. Abrasion grooves as well as fine wear debris are seen, indicating that three-body abrasion also takes place, but due to the small scale of the particles, its contribution to wear is minor. EDS results showed strong peaks of oxygen and iron, but also, indicates the presence of C. GO is exfoliated on the contact, contributing to form a tribo-layer that exhibited lower friction and wear. Besides, C is detected only on the oxide film areas. Oxide film helps to retain exfoliated GO in the surface.

The improved tribological performance of Co composite coatings using 0.2 and 0.3 g/L of ZnO@GO addition is owing to the formation of an easy-shear oxide film, containing exfoliated GO, on the wear track. Moreover, it should be mentioned that despite there was no evidence of Zn on the wear track at the end of the test, ZnO nanoparticles could also have participated at the early stages, acting as load bearing and its effect as dispersion strengthening hinders dislocation movement. Qi et al. [23] reported the formation of oxide layer along with GO exfoliation for Ni/GO composites, which reduced in low friction coefficients.

4. Conclusions

In this study, the tribological behavior of CPED deposited pure Co and Co/ZnO@GO composite coatings sliding against AISI 52100 steel ball were evaluated. CPED sucessfuly produced nanostructured coatings, with high hardness and nanoparticle addition reduced surface roughness. It was observed that the incorporation of ZnO@GO core-shell nanoparticles with a content superior to 0.2 g/L can effectively increase hardness and decrease friction and wear. An oxide tribolayer was formed in all coatings, supressing friction and for higher contents of ZnO@GO, this layer entrapped exfoliated GO on the wear track, further decreasing friction and wear.

Declaration of competing interest

The authors declare that they have no known competing financial interests or personal relationships that could have appeared to influence the work reported in this paper.

References

[1] D. Landolt, Electrochemical and materials science aspects of alloy deposition, Electrochim. Acta 39 (8–9) (1994) 1075–1090, https://doi.org/10.1016/0013-4686(94)E0022-R.

[2] S. Mahdavi, S.R. Allahkaram, Characteristics of electrodeposited cobalt and titania nano-reinforced cobalt composite coatings, Surf. Coating. Technol. 232 (2013) 198–203, https://doi.org/10.1016/j.surfcoat.2013.05.007.

[3] K.M. Hyie, N.A. Resali, W.N.R. Abdullah, W.T. Chong, Synthesis and characterization of nanocrystalline pure cobalt coating: effect of pH, Procedia Eng. 41 (2012) 1627–1633, https://doi.org/10.1016/j.proeng.2012.07.360.

[4] E.V. Parfenov, A. Yerokhin, R.R. Nevyantseva, M.V. Gorbatkov, C.J. Liang, A. Matthews, Towards smart electrolytic plasma technologies: an overview of methodological approaches to process modelling, Surf. Coating. Technol. 269 (2015) 2–22, https://doi.org/10.1016/j.surfcoat.2015.02.019.

[5] T. Paulmier, J.M. Bell, P.M. Fredericks, Development of a novel cathodic plasma/electrolytic deposition technique: Part 2: physico-chemical analysis of the plasma discharge, Surf. Coating. Technol. 201 (21) (2007) 8771–8781, https://doi.org/10.1016/j.surfcoat.2006.07.066.

[6] D.P. Weston, P.H. Shipway, S.J. Harris, M.K. Cheng, Friction and sliding wear behaviour of electrodeposited cobalt and cobalt–tungsten alloy coatings for replacement of electrodeposited chromium, Wear 267 (5–8) (2009) 934–943, https://doi.org/10.1016/j.wear.2009.01.006.

[7] C.B. Wang, D.L. Wang, W.X. Chen, Y.Y. Wang, Tribological properties of nanostructured WC/CoNi and WC/CoNiP coatings produced by electro-deposition, Wear 253 (5–6) (2002) 563–571, https://doi.org/10.1016/S0043-1648(02)00173-4.

[8] F. Su, C. Liu, P. Huang, Friction and wear of nanocrystalline Co and Co–W alloy coatings produced by pulse reverse electrodeposition, Wear 300 (1–2) (2013) 114–125, https://doi.org/10.1016/j.wear.2013.01.120.

[9] L. Wang, Y. Gao, T. Xu, Q. Xue, A comparative study on the tribological behavior of nanocrystalline nickel and cobalt coatings correlated with grain size and phase structure, Mater. Chem. Phys. 99 (1) (2006) 96–103, https://doi.org/10.1016/j.matchemphys.2005.10.014.

[10] E. Rudnik, L. Burzyńska, M. Gębka, Influence of CTAB cationic surfactant on codeposition of SiC particles with cobalt, Transactions of the IMF 89 (1) (2011) 33–38, https://doi.org/10.1179/174591910X12835095635187.

[11] C. Liu, F. Su, J. Liang, Producing cobalt–graphene composite coating by pulse electrodeposition with excellent wear and corrosion resistance, Appl. Surf. Sci. 351 (2015) 889–896, https://doi.org/10.1016/j.apsusc.2015.06.018.

[12] S. Mahdavi, A. Asghari-Alamdari, M. Zolola-Meibodi, Effect of alumina particle size on characteristics, corrosion, and tribological behavior of Co/Al2O3 composite coatings, Ceram. Int. 46 (4) (2020) 5351–5359, https://doi.org/10.1016/j.ceramint.2019.10.289.

[13] A. Toosinezhad, M. Alinezhadfar, S. Mahdavi, Cobalt/graphene electrodeposits: characteristics, tribological behavior, and corrosion properties, Surf. Coating. Technol. 385 (2020), 125418, https://doi.org/10.1016/j.surfcoat.2020.125418.

[14] S. Arai, K. Miyagawa, Frictional and wear properties of cobalt/multiwalled carbon nanotube composite films formed by electrodeposition, Surf. Coating. Technol. 235 (2013) 204–211, https://doi.org/10.1016/j.surfcoat.2013.07.034.

[15] Y.G. Zhang, W.C. Sun, M. Ma, S.S. Tian, Y.W. Liu, Y. Xiao, Deposition characteristics, microstructure and wear behaviour of Co–WC composite coatings, Surf. Eng. 37 (6) (2021) 702–711, https://doi.org/10.1080/02670844.2020.1840694.

[16] J. Huang, J. Zhu, X. Fan, D. Xiong, J. Li, Preparation of MoS2-Ti (C, N)-TiO2 coating by cathodic plasma electrolytic deposition and its tribological properties, Surf. Coating. Technol. 347 (2018) 76–83, https://doi.org/10.1016/j.surfcoat.2018.04.059.

[17] C. Liu, S. Zhang, R. Ji, P. Wang, J. Zhang, Y. Tian, Y. He, Cathode plasma electrolytic deposition of Al2O3 coatings doped with SiC particles, Ceram. Int. 45 (4) (2019) 4747–4755, https://doi.org/10.1016/j.ceramint.2018.11.167.

[18] C. Quan, S. Deng, Y. Jiang, C. Jiang, M. Shuai, Characteristics and high temperature oxidation behavior of Ni-Cr-Y2O3 nanocomposite coating prepared by cathode plasma electrolytic deposition, J. Alloys Compd. 793 (2019) 170–178, https://doi.org/10.1016/j.jallcom.2019.04.063.

[19] W.S. Hummers Jr., R.E. Offeman, Preparation of graphitic oxide, J. Am. Chem. Soc. 80 (6) (1958), https://doi.org/10.1021/ja01539a017, 1339-1339.

[20] Y.N. Baghdadi, L. Youssef, K. Bouhadir, M. Harb, S. Mustapha, D. Patra, A. R. Tehrani-Bagha, The effects of modified zinc oxide nanoparticles on the mechanical/thermal properties of epoxy resin, J. Appl. Polym. Sci. 137 (43) (2020), 49330, https://doi.org/10.1002/app.49330.

[21] J. Hong, C. Liu, X. Deng, T. Jiang, L. Gan, J. Huang, Enhanced tribological properties in core–shell structured SiO 2@ GO hybrid fillers for epoxy nanocomposites, RSC Adv. 6 (92) (2016) 89221–89230, https://doi.org/10.1039/C6RA18207K.

[22] M. Sajjadnejad, S.M.S. Haghshenas, V.T. Targhi, N. Setoudeh, A. Hadipour, A. Moghanian, S. Hosseinpour, Wear behavior of alkaline pulsed electrodeposited nickel composite coatings reinforced by ZnO nanoparticles, Wear 468 (2021), 203591, https://doi.org/10.1016/j.wear.2020.203591.
[23] S. Qi, X. Li, H. Dong, Reduced friction and wear of electro-brush plated nickel composite coatings reinforced by graphene oxide, Wear 426 (2019) 228–238, https://doi.org/10.1016/j.wear.2018.12.069.
[24] P. Shankar, M.H. Ishak, J.K. Padarti, N. Mintcheva, S. Iwamori, S.O. Gurbatov, S. A. Kulinich, ZnO@ graphene oxide core@ shell nanoparticles prepared via one-pot approach based on laser ablation in water, Appl. Surf. Sci. 531 (2020), 147365, https://doi.org/10.1016/j.apsusc.2020.147365.
[25] B. Ren, L. Gao, M. Li, S. Zhang, X. Ran, Tribological properties and anti-wear mechanism of ZnO@ graphene core-shell nanoparticles as lubricant additives, Tribol. Int. 144 (2020), 106114, https://doi.org/10.1016/j.triboint.2019.106114.
[26] S.S.P. Haghshenas, A. Nemati, R. Simchi, C.U. Kim, Photocatalytic and photoluminescence properties of ZnO/graphene quasi core-shell nanoparticles, Ceram. Int. 45 (7) (2019) 8945–8961, https://doi.org/10.1016/j.ceramint.2019.01.226.
[27] P. Gupta, G. Tenhundfeld, E.O. Daigle, D. Ryabkov, Electrolytic plasma technology: science and engineering—an overview, Surf. Coating. Technol. 201 (21) (2007) 8746–8760, https://doi.org/10.1016/j.surfcoat.2006.11.023.
[28] C. Quan, Y. He, Microstructure and characterization of a novel cobalt coating prepared by cathode plasma electrolytic deposition, Appl. Surf. Sci. 353 (2015) 1320–1325, https://doi.org/10.1016/j.apsusc.2015.07.080.